INFECTION AND IMMUNITY, Dec. 2003, p. 6830–6834 Vol. 71, No. 12
0019-9567/03/$08.00+0 DOI: 10.1128/IAI.71.12.6830–6834.2003

The Site of *Leishmania major* Infection Determines Disease Severity and Immune Responses

Tracey M. Baldwin, Colleen Elso, Joan Curtis, Lynn Buckingham, and Emanuela Handman*

The Walter and Eliza Hall Institute of Medical Research, Melbourne, Australia

Received 9 June 2003/Returned for modification 2 August 2003/Accepted 30 August 2003

Inbred strains of mice infected with *Leishmania major* have been classified as genetically resistant or susceptible on the basis of their ability to cure their lesions, the parasite burden in the draining lymph nodes, and their type of T helper cell immune responses to the parasite. Using the intradermal infection at the base of the tail and the ear pinna, we compared for the first time the above-mentioned parameters in six strains of mice infected with metacyclic promastigotes, and we show that the severity of disease depends greatly on the site of infection. Although the well-documented pattern of disease susceptibility of BALB/c and C57BL/6 mice described for the footpad and base-of-the-tail models of leishmaniasis were confirmed, C3H/HeN and DBA/2 mice, which are intermediate and susceptible, respectively, in the tail and other models, were resistant to ear infection. Moreover, in the CBA/H, C3H/HeN, C57BL/6J, and DBA/2 mouse strains, there was little correlation between the pattern of cytokines produced and the disease phenotype observed at the ear and tail sites. We conclude that the definition of susceptibility and the immune mechanisms leading to susceptibility or resistance to infection may differ substantially depending on the route of infection.

The clinical manifestations of human cutaneous leishmaniasis caused by *Leishmania major*, *Leishmania tropica*, and *Leishmania mexicana* display a spectrum of disease severity (7). Although it is generally accepted that pathogenicity and virulence must be understood in terms of the interaction between the individual genotypes of the microorganism and its host, dissecting out the relative contributions has been difficult, especially in outbred host populations, such as humans (8, 24). In the case of leishmaniasis, this problem has been addressed with a reasonable degree of success by using inbred strains of mice in which the various disease phenotypes resemble the spectrum of clinical manifestations in humans.

The disease phenotype observed in human cutaneous leishmaniasis can be mimicked in the laboratory by infection of different inbred strains of mice with *L. major* (18). Thus, the mouse model of the highly susceptible BALB/c mouse at one end of the spectrum and the resistant C57BL/6J mouse at the other has been widely used to study both the genetics and biology of the host response to infection. In this system, the marked polarization in the immune response observed upon challenge with *L. major* parasites has been implicated in determining the severity of disease. BALB/c mice produce Th2-type cytokines, in particular interleukin-4 (IL-4), which has been shown to be associated with disease progression and susceptibility (12, 18). In contrast, recovery from infection in resistant C57BL/6J mice depends upon the induction of a Th1-type response resulting in activation of macrophages and killing of the intracellular organisms (3, 22). However, in the case of SWR mice, the cytokine profile was not predictive of the disease outcome (11).

Other factors have also been shown to influence the disease phenotype and, by inference, susceptibility or resistance. The size of the inoculum (4, 16) and the strain of the parasite used (10, 11), as well as the site of infection, seem to be particularly important (11). For example, SWR mice are similar in susceptibility to BALB/c mice and develop large lesions upon infection at the base of the tail, but unlike the BALB/c mice, they are able to cure the lesions generated by footpad infection (14). Interestingly, in these mice, unlike the BALB/c mice, the cytokine profile was not predictive of the disease outcome.

There is now significant evidence that infection of mice by inoculation at the base of the tail or in the footpad with large numbers of parasites does not reflect the situation during the natural course of the disease, where small numbers of the virulent metacyclic forms are introduced by the sandfly. Belkaid and colleagues have established a new model for cutaneous leishmaniasis which resembles the natural infection more closely; it involves intradermal infection in the pinna of the ear of BALB/c or C57BL/6 mice with small numbers of virulent metacyclic promastigotes (1, 2).

In previous studies, stationary-phase promastigote infection at the base of the tail and mice of intermediate susceptibility to infection, such as C3H/HeN mice, were used because they provide a wider time window for observation (9). We chose this strain because we considered that neither the highly susceptible BALB/c mice nor the highly resistant C57BL/6J mice are representative of the bulk of the human population, which is more like the intermediately susceptible mice. In preparation to changing our experimental system to the ear–metacyclic-promastigote model of infection, we have undertaken tail and ear inoculations with *L. major* Friedlin VI, as described by Belkaid and colleagues and Sacks and Noben-Trauth (1, 18), to compare the pattern of lesion development in several commonly used inbred strains of mice. Our results reveal a previously unsuspected level of complexity even when a cloned parasite line is used and show that conclusions regarding disease susceptibility and the adaptive immune responses induced

* Corresponding author. Mailing address: The Walter and Eliza Hall Institute of Medical Research, 1G Royal Parade, Parkville, Victoria 3050, Australia. Phone: 61-3-9345-2476. Fax: 61-3-9347-0852. E-mail: handman@wehi.edu.au.

TABLE 1. Primers used in this study

Target	Forward primer	Reverse primer	$MgCl_2$ (mM)	Melting temp (°C)	Product size (bp)
PBGD[a]	CCTGGTTGTTCACTCCCTGA	CAACAGCATCACAAGGGTTTT	3	84.4	98
IL-4	TTTTGAACGAGGTCACAGGA	AGCCCTACAGACGAGCTCAC	3	86.9	107
IFN-γ	CTTCTTCAGCAACAGCAAGG	TGAGCTCATTGAATGCTTGG	3	84.7	101

[a] PBGD, porphobilinogen deaminase.

by infection are highly dependent on the experimental model that is used.

MATERIALS AND METHODS

Animals. BALB/c, C3H/HeN, C57BL/6J, CBA/H, DBA/2, and (C57BL/6J × BALB/c)F_1 female mice aged 6 to 7 weeks were obtained from the specific-pathogen-free animal-breeding facility at The Walter and Eliza Hall Institute of Medical Research and maintained in a conventional animal facility.

Parasites. The parasites used were the cloned line Friedlin VI derived from the *L. major* human isolate MHOM/IL/80/Friedlin (a kind gift from D. L. Sacks). Promastigotes were maintained in vitro at 26°C in Schneider's *Drosophila* medium or in M199 medium supplemented with 10% fetal bovine serum (HyClone, Logan, Utah). For infection of mice, the parasites were grown in biphasic blood agar medium (15). In order to maintain virulent stocks of *L. major*, the parasites were maintained in mice and cultured for a maximum of 4 weeks.

Infection and monitoring of the disease pattern. Metacyclic promastigotes were prepared according to the method of Courret et al. (6) from 6-day-old cultures by selection of parasites which did not agglutinate with 100 μg of peanut agglutinin (Vector Laboratories)/ml. Using intradermal injection, 10^4 promastigotes were administered to mice in a 10-μl volume (19, 20). Lesion development was assessed weekly by measuring the diameter of the lesion, as described previously (13).

A statistical permutation was utilized to compare the mean lesion scores of paired mouse strains over the entire course of the infection. Briefly, the test statistic (ave.t) was the two-sample t statistic used to compare the average lesion scores of two groups each week throughout the course of the infection. A *P* value was obtained for the test statistic by simulation. Mice were randomly allocated to one of the two groups, and ave.t was recalculated for 10,000 data sets permuted in this way. The *P* value is the proportion of permutations where the absolute value of ave.t was greater than that of ave.t for the original subset. Pairwise comparisons were performed among the six mouse strains, resulting in 15 pairwise tests and *P* values. The 15 *P* values were adjusted for multiple testing using a step-down Bonferonni procedure (21). A *P* value of <0.05 was considered significant.

Limiting-dilution analysis of parasite burden. At 5, 10, and 15 weeks postinfection, draining lymph nodes from at least two mice in each group were taken for analysis. One of the two lymph nodes was used for analysis of cytokine production by quantitative PCR, and the second was used to determine the parasite burden by limiting-dilution analysis as described previously (23).

Cytokine production. Analysis of IL-4 and gamma interferon (IFN-γ) mRNA expression was carried out using the real-time fluorescence PCR assay described by Elso et al. (7a). Real-time fluorescence PCR assays were carried out on the LightCycler (Roche Molecular Biochemicals, Basel, Switzerland) using the Fast-start DNA Master SYBR Green kit (Roche Molecular Biochemicals) with the primers for IL-4, IFN-γ, and the housekeeping gene for porphobilinogen deaminase (5). This housekeeping gene was chosen because it is a single-copy gene with no pseudogenes and it is expressed at low levels, similar to cytokine expression. High-performance liquid chromatography-purified primers were obtained from Sigma Genosys. The primers and expected product sizes are listed in Table 1. For each assay, the PCR conditions were 10 min at 95°C, followed by 40 cycles of 10 s at 95°C, 5 s at 60°C, and 4 s at 72°C.

RESULTS AND DISCUSSION

The model of murine cutaneous leishmaniasis using small numbers of metacyclic promastigotes injected strictly intradermally into the pinna of the ear, described by Belkaid and colleagues and Sacks and Noben-Trauth, is a very attractive system to examine issues such as innate and adaptive immune responses and, in our case, the genetic basis for susceptibility to disease (1, 2, 18).

In this study, we compared the disease patterns, the parasite burdens, and the cytokine profiles of five commonly used inbred mouse strains, BALB/c, C57BL/6J, C3H/HeN, CBA/H, and DBA/2, plus an F_1 hybrid derived from a genetic cross between C57BL/6J and BALB/c. All received 10^4 *L. major* Friedlin VI metacyclic promastigotes as either an intradermal ear or base-of-tail injection.

Courses of disease in various mouse strains infected with Friedlin VI in ear pinna and base of the tail. From two experiments in which mice were infected in the ear pinna, the mice could be ranked in four groups on the basis of the pattern of lesion development (Fig. 1A and 2A). BALB/c mice were highly susceptible, and (C57BL/6J × BALB/c)F_1 mice showed intermediate susceptibility. C57BL/6J mice were classified as resistant, with moderate swelling 4 weeks after infection and complete healing in all mice by week 15 (Fig. 1A). The strains C3H/HeN, CBA/H, and DBA/2 were characterized as highly resistant. The severity of disease was greatest in the BALB/c mice, where initial small lesions developed into nonhealing, large, open ulcers as the course of infection progressed (Fig. 1A). As anticipated, the F_1 mice developed a disease pattern which was intermediate between the two parental extremes (17). The F_1 mice developed moderate swelling within 4 weeks, and this continued to be present throughout the remainder of the experiment (Fig. 2A). The highly resistant CBA/H (Fig. 2A) and C3H/HeN (Fig. 1A) mice developed a slightly roughened area on the skin 3 weeks postinfection, but this cleared by week 10, while the DBA/2 mice developed a very small papule which also healed by week 10 (Fig. 2A).

In the experimental tail infections, the BALB/c mice were also highly susceptible and the F_1 mice demonstrated intermediate susceptibility. In this case, though, the DBA/2 mice, as well as the C57BL/6J and C3H/HeN mice, were classified as resistant, and only the CBA/H mice were characterized as highly resistant. As was the case with the infection in the ear, the greatest disease severity was observed in the BALB/c mice, where early lesion development progressed to a nonhealing, large, ulcerated sore over the course of infection (Fig. 1D). The intermediately susceptible F_1 mice developed a small lesion immediately after infection, which progressed by week 4 to a moderate but nonhealing lesion (Fig. 2D). The resistant C57BL/6J mice infected at the base of the tail developed small swellings 3 to 4 weeks postinfection, but these healed by week 10 (Fig. 1D). The C3H/HeN mice produced small lesions, but they healed more slowly than those of the C57BL/6J mice (Fig. 1D). The highly resistant CBA/H mice (Fig. 2D) developed small nodules within the first 4 weeks, and these resolved by week 8 postinfection. The DBA/2 mice developed a very dif-

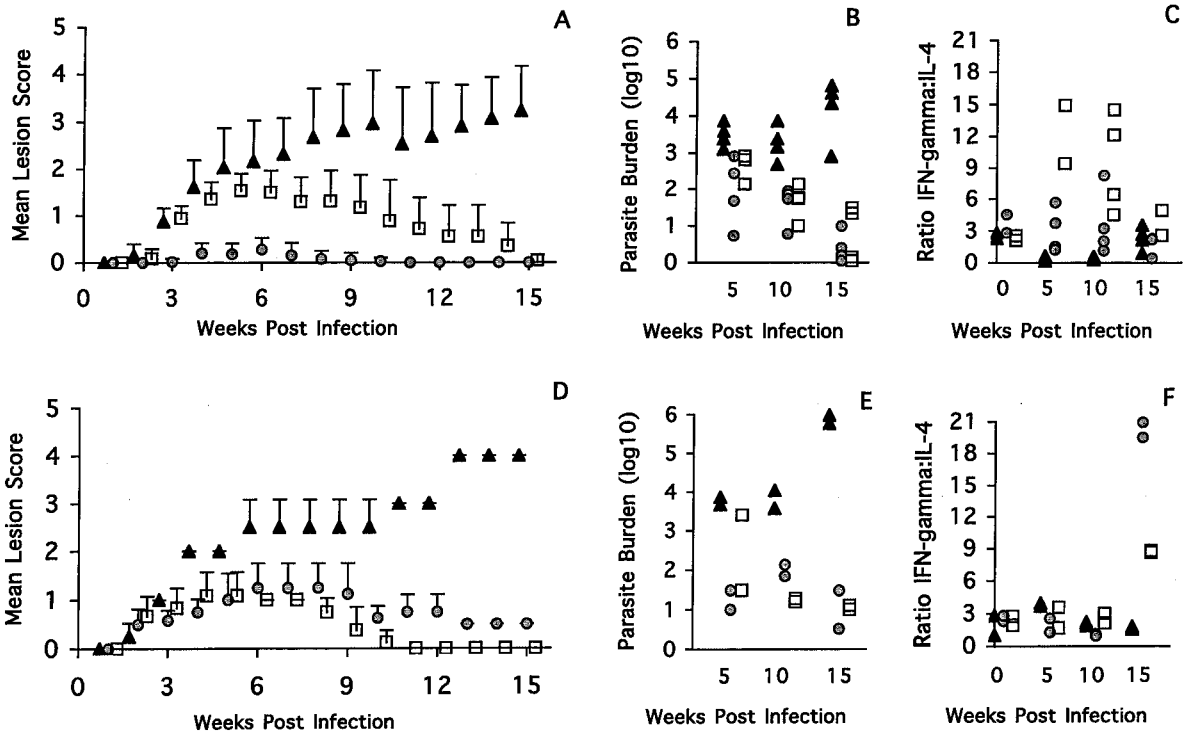

FIG. 1. (A and D) Disease patterns in BALB/c (triangles), C3H/HeN (circles), and C57BL/6J (squares) mice infected intradermally in the ear (A) or tail (D) with 10^4 *L. major* Friedlin metacyclic promastigotes. The means and standard deviations of the lesion scores are shown as a function of time. (B and E) Parasite burden per 10^6 lymph node cells in individual mice tested at 5, 10, and 15 weeks after infection with 10^4 *L. major* Friedlin metacyclic promastigotes in the ear (B) or tail (E). (C and F) Ratios of IFN-γ to IL-4 in individual mice tested at 0, 5, 10, and 15 weeks post infection with 10^4 *L. major* Friedlin metacyclic promastigotes in the ear (C) or tail (F).

ferent disease pattern when infected at the base of the tail than when infected in the ear (Fig. 2D). Initially, the lesions on the DBA/2 mice appeared to advance slowly, but by week 5 to 6 postinfection, the mice had moderate or large open ulcers which did not heal after 15 weeks. This is in contrast to the disease pattern in the ear, where the DBA/2 mice developed minimal lesions (Fig. 2A).

In order to evaluate more quantitatively the differences among the various mouse strains, a statistical permutation was used to compare the mean lesion scores of paired mouse strains over the entire course of the infection. The data from the statistical analysis indicate that in the ear model, differences were significant for all pairwise comparisons ($P = 0.0000$ to 0.0300; $n = 6$ to 8) except for the BALB/c and (C57BL/6J × BALB/c)F_1 pair ($P = 0.0510$; $n = 6$ to 8) and the C3H/HeN and CBA/H pair ($P = 0.0812$; $n = 8$), confirming the conclusions reached by direct measurements of the lesions. In the tail model, the differences were also statistically significant for all pairs compared, with an adjusted P value of 0.0000 to 0.0116 ($n = 6$).

From the statistical permutation data, a resistant-to-susceptible ranking system was used for the ear and tail models based on the severity of the observed lesions. In the ear model, the mice were ranked as follows: CBA/H = C3H/HeN > DBA/2 > C57BL/6J > F_1 > BALB/C. The base-of-the-tail model showed a quite different ranking: CBA/H > C57BL/6J > C3H/HeN > F_1 > DBA/2 > BALB/c, indicating that the site of infection plays a major role in the ensuing disease pathology.

The relationship between disease pattern and parasite burden in mice infected in the ear pinna and base of the tail. The size of the lesion that develops at the site of infection may reflect the parasite burden or the degree of tissue damage caused by the host immune response to the parasite. Therefore, we set out to quantitate the parasite burdens in the lymph nodes draining the lesion 5, 10, and 15 weeks postinfection and correlate them with the sizes of the lesions.

Among the mouse strains examined, the BALB/c mice had the greatest parasite load 5 weeks postinfection by intradermal ear or tail injection. This load was maintained at week 10 but increased further at week 15 (Fig. 1B and E), thus providing a direct correlation between the disease pattern and the parasite load. In both the ear and tail systems, the C57BL/6J mice showed at least a log-unit-lower parasite load at week 5 than the BALB/c mice. This load declined further throughout the course of infection, reflecting the healing of the lesions (Fig. 1B and D). In the C3H/HeN and CBA/H mice infected in the ear, there was an early parasite burden in the draining lymph nodes, which declined over time (Fig. 1B and 2B). The resultant parasite load and minimal lesion development shown by these mouse strains suggests that they are the most resistant. In contrast, there was no correlation between the lesion and the parasite burden in the C3H/HeN and CBA/H mice infected at the tail site. In both strains, the lesions appeared to be healing (C3H/HeN) or resolved (CBA/H), yet the parasite loads peaked at week 10 before declining at week 15 (Fig. 1E and 2E).

In both disease models examined, for the (C57BL/6J × BALB/c)F_1 mice, the lesion sizes and parasite loads correlated well during the period of observation (Fig. 2B and 2E). The only exception was the range of parasite burdens recorded for

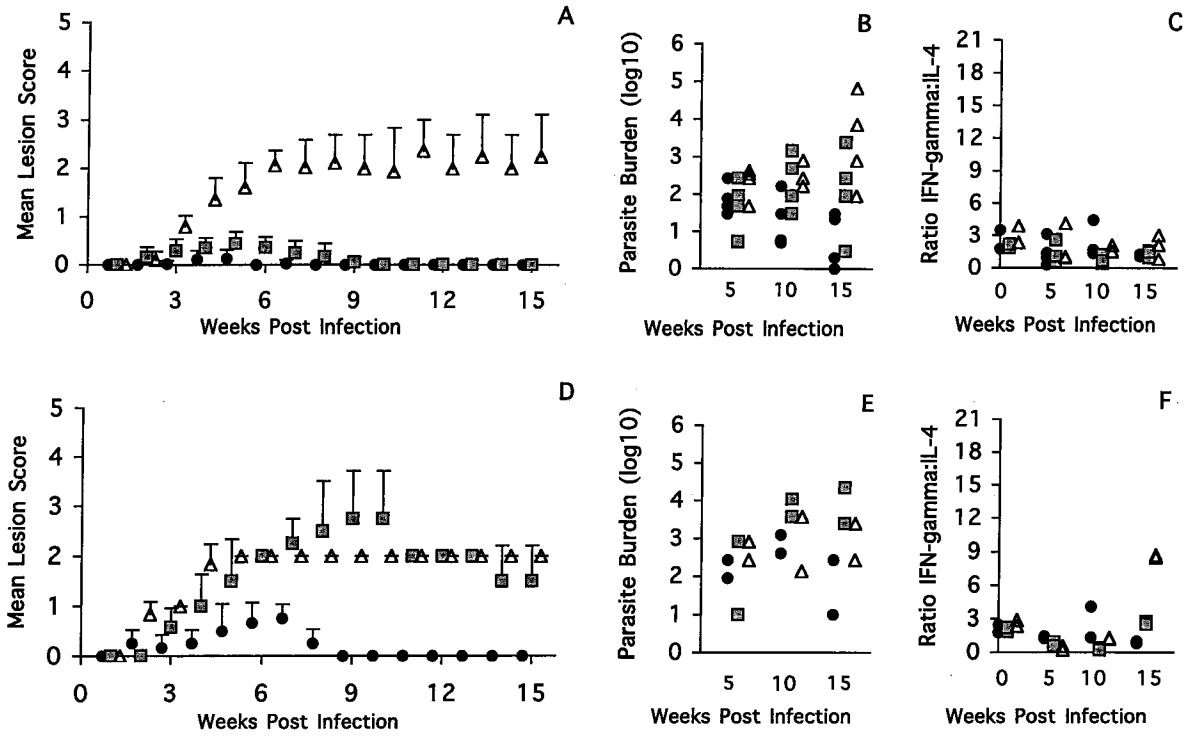

FIG. 2. (A and D) Disease pattern in CBA/H (circles), DBA/2 (squares), and (C57BL/6J × BALB/c)F_1 (triangles) mice infected intradermally in the ear (A) or tail (D) with 10^4 *L. major* Friedlin metacyclic promastigotes. The mean lesion scores and standard deviations are shown as a function of time. (B and E) Parasite burden at 5, 10, and 15 weeks after infection with 10^4 *L. major* Friedlin metacyclic promastigotes in the ear (B) or tail (E) are shown as in Fig. 1. (C and F) Ratio of IFN-γ to IL-4 at 0, 5, 10, and 15 weeks postinfection with 10^4 *L. major* Friedlin metacyclic promastigotes in the ear (C) or tail (F) is shown as in Fig. 1.

the week 15 ear infections. This result may be a reflection of the variability in the size of the lesion, which was also a feature of the F_1 mice (Fig. 2A).

In the case of the DBA/2 mice infected in the ear, the parasite load did not correlate with the size of the lesion (Fig. 2B). In general, the parasite burden increased slowly throughout the course of infection, despite the lack of detectable ear lesions after week 9 (Fig. 2B). In contrast, in the DBA/2 mice infected at the base of the tail (Fig. 2E), the parasite load appeared fairly constant throughout the course of the infection. Here, a steady state appears to have been reached between the nonhealing lesions and the parasite load.

Relationship between disease pattern and cytokine profile in mice infected in the ear pinna and base of the tail. In parallel with the analysis of the parasite load in one draining lymph node, we examined the contralateral node for the presence of mRNA encoding the signature Th1 and Th2 cytokines IFN-γ and IL-4 throughout the course of infection. The levels of cytokine production in the various mouse strains were quantitated using real-time fluorescence PCR before infection at time zero and at weeks 5, 10, and 15 postinfection and were expressed as the mean ratio of IFN-γ to IL-4.

The mice that were injected in the ear pinna (Fig. 1C and 2C) showed the following cytokine responses. The BALB/c mice showed a predominantly Th2 response at weeks 5 and 10, with a shift toward greater IL-4 production. Surprisingly, at week 15, a time when the lesions were large and the parasite burden was high, the cytokine ratio returned to a value similar to that in the baseline controls (Fig. 1C). The C57BL/6J mice showed the most marked Th1-type response (Fig. 1C). The ratio of IFN-γ to IL-4 rose above those in the other strains but declined by week 15 as the lesions healed. In contrast, the production of the Th1-type cytokines in C3H/HeN mice was low despite their obvious resistance to disease pathology (Fig. 1C). In these mice, there appeared to be a small increase in the ratio of IFN-γ to IL-4 at week 5, but this returned to baseline levels by week 10. The CBA/H, DBA/2, and (C57BL/6J × BALB/c) F_1 mice all had low ratios of IFN-γ to IL-4 at weeks 5, 10, and 15 postinfection which were similar to those in the uninfected controls (Fig. 2C). In the case of the F_1 mice, this result correlates well with the parasite load and disease pattern. However, for the CBA/H and DBA/2 mice, such results reflected the parasite load but not the severity of lesion pathology.

For the mice infected at the base of the tail, the cytokine responses in the BALB/c mice (Fig. 1F and 2F) show a very low ratio of IFN-γ to IL-4 at week 5 of infection, with a return to baseline by week 10, when the lesions were large and the parasite burdens were high. In the case of the C3H/HeN and C57BL/6J mice, both infected and control mice had similarly low ratios of IFN-γ to IL-4 at weeks 5 and 10 postinfection (Fig. 1F). Interestingly, the polarized Th1 pattern of cytokine production observed in the C57BL/6J ear model (Fig. 1C) was not detected in the C57BL/6J tail model until late in the course of the infection (week 15), when the lesions had already healed. A significant increase in the ratio of IFN-γ to IL-4 was also observed in the C3H/HeN mice, which may reflect the

final push toward clearance of the lesion. Notably, it is possible that the peak of cytokine mRNA production in these mice may have arisen much earlier in the tail model than in that of the ear. Like the C57BL/6J mice, the F_1 mice infected at the base of the tail also had a late Th1-type cytokine response, which was unexpected given that at weeks 5 and 10 postinfection the immune response appeared to be skewed toward a Th2 response, which correlated well with the disease pattern and parasite load observed (Fig. 2F). Throughout the course of the experiment, the DBA/2 mice had a very low ratio of IFN-γ to IL-4, suggesting that some association exists among the three parameters examined (Fig. 2F). In comparison, the relationship among these parameters was inconsistent in the tail model of the CBA/H mice (Fig. 2F). Moreover, although the CBA/H mice cured their lesions quite rapidly, the ratio of IFN-γ to IL-4 appeared to remain below the threshold of the CBA/H baseline control (Fig. 2F).

Although in the BALB/c, C57BL/6J, and F_1 mouse strains, the pattern of lesion size and development (Fig. 1A and D and 2A and D) and parasite load (Fig. 1B and E and 2B and E) correlated well throughout the course of the infection, the associated cytokine production did not always reflect the severity of the disease. Moreover, for the C3H/HeN, CBA/H, and DBA/2 mice, not only was there a lack of correlation between the overall disease pattern in the base-of-tail and ear models, there also seemed to be little correlation among the three parameters measured: lesion size, parasite burden, and cytokine production. The most striking situation was observed in the C3H/HeN and CBA/H mice, where it appears that there may be mechanisms distinct from T helper cell-mediated responses which account for the apparent resistance to infection as determined by lesion size.

In conclusion, this study compares for the first time two experimental models for cutaneous leishmaniasis in several commonly used strains of mice in terms of three parameters: the gross pathology at the site of infection, parasite clearance, and the immune responses which may affect the disease phenotype. The conclusions from this study are that the site of infection plays a critical role in determining not only the pathology but also the immune responses induced by infection. Moreover, depending on the site of infection, these responses do not always correlate with the severity of disease as measured by lesion size or parasite burden. These conclusions are important when choosing a model for the study of genetic susceptibility to infection, adaptive immune responses, or vaccine development. Finally, the data highlight a dilemma: which animal model more closely resembles the situation in the human disease?

ACKNOWLEDGMENTS

We thank Gordon Smyth for creating the statistical program required to analyze our data and Jim Goding for his critical review of the manuscript.

This work was supported by the National Health and Medical Research Council of Australia and by the UNDP/World Bank/WHO Special Programme for Research and Training in Tropical Diseases (TDR).

REFERENCES

1. **Belkaid, Y., S. Kamhawi, G. Modi, J. Valenzuela, N. Noben-Trauth, E. Rowton, J. Ribeiro, and D. L. Sacks.** 1998. Development of a natural model of cutaneous Leishmaniasis: powerful effects of vector saliva and saliva preexposure on the long-term outcome of *Leishmania major* infection in the mouse ear dermis. J. Exp. Med. **188:**1941–1953.
2. **Belkaid, Y., S. Mendez, R. Lira, N. Kadambi, G. Milon, and D. Sacks.** 2000. A natural model of *Leishmania major* infection reveals a prolonged "silent" phase of parasite amplification in the skin before the onset of lesion formation and immunity. J. Immunol. **165:**969–977.
3. **Biedermann, T., S. Zimmermann, H. Himmelrich, A. Gumy, O. Egeter, A. K. Sakrauski, I. Seegmuller, H. Voigt, P. Launois, A. D. Levine, H. Wagner, K. Heeg, J. A. Louis, and M. Rocken.** 2001. IL-4 instructs TH1 responses and resistance to *Leishmania major* in susceptible BALB/c mice. Nat. Immunol. **2:**1054–1060.
4. **Bretscher, P. A., G. Wei, J. N. Menon, and H. Bielefeldt-Ohmann.** 1992. Establishment of stable, cell-mediated immunity that makes "susceptible" mice resistant to *Leishmania major*. Science **257:**539–542.
5. **Chretien, S., A. Dubart, D. Beaupain, N. Raich, B. Grandchamp, J. Rosa, M. Goossens, and P. H. Romeo.** 1988. Alternative transcription and splicing of the human porphobilinogen deaminase gene result either in tissue-specific or in housekeeping expression. Proc. Natl. Acad. Sci. USA **85:** 6–10.
6. **Courret, N., E. Prina, E. Mougneau, E. M. Saraiva, D. L. Sacks, N. Glaichenhaus, and J. C. Antoine.** 1999. Presentation of the *Leishmania* antigen LACK by infected macrophages is dependent upon the virulence of the phagocytosed parasites. Eur. J. Immunol. **29:**762–773.
7. **Desjeux, P., S. Mollinedo, F. Le Pont, A. Paredes, and G. Ugarte.** 1987. Cutaneous leishmaniasis in Bolivia. A study of 185 human cases from Alto Beni (La Paz Department). Isolation and isoenzyme characterization of 26 strains of *Leishmania braziliensis braziliensis.* Trans. R. Soc. Trop. Med. Hyg. **81:**742–746. (Erratum, **82:**83, 1988.)

7a. **Elso, C., L. J. Roberts, G. K. Smyth, R. J. Thomson, T. M. Baldwin, S. J. Foote, and E. Handman.** Leishmaniasis host response loci (lmr1, 2, and 3) modify disease severity through a Th1/Th2 independent pathway. Genes Immun., in press.

8. **Greenblatt, C. L.** 1980. The present and future of vaccination for cutaneous leishmaniasis. Prog. Clin. Biol. Res. **47:**259–285.
9. **Handman, E.** 2001. Leishmaniasis: current status of vaccine development. Clin. Microbiol. Rev. **14:**229–243.
10. **Kebayer, C., H. Louzir, M. Chenik, A. Ben Saleh, and K. Delaggi.** 2001. Heterogeneity of wild *Leishmania major* isolates in experimental murine pathogenicity and specific immune responses. Infect. Immun. **69:**4906–4915.
11. **Kirkpatrick, C. E., T. J. Nolan, and J. P. Farrell.** 1987. Rate of *Leishmania*-induced skin-lesion development in rodents depends on the site of inoculation. Parasitology **94:**451–465.
12. **Locksley, R. M., F. P. Heinzel, M. D. Sadick, B. J. Holaday, and K. J. Gardner.** 1987. Murine cutaneous leishmaniasis: susceptibility correlates with differential expansion of helper T-cell subsets. Ann. Inst. Pasteur Immunol. **138:**744–749.
13. **Mitchell, G. F.** 1983. Murine cutaneous leishmaniasis: resistance in reconstituted nude mice and several F1 hybrids infected with *Leishmania tropica major.* J. Immunogenet. **10:**395–412.
14. **Nabors, G. S., and J. P. Farrell.** 1994. Site-specific immunity to *Leishmania major* in SWR mice: the site of infection influences susceptibility and expression of the antileishmanial immune response. Infect. Immun. **62:**3655–3662.
15. **Nicolle, C. H.** 1908. Cultures des corps de Leishman isoles de la rate dans trois cas d'anemie splenique infantile. Bull. Soc. Pathol. Exot. **1:**121.
16. **Preston, P. M., and D. C. Dumonde.** 1976. Experimental cutaneous leishmaniasis. V. Protective immunity in subclinical and selfhealing infection in the mouse. Clin. Exp. Immunol. **23:**126–138.
17. **Roberts, L. J., T. M. Baldwin, J. M. Curtis, E. Handman, and S. J. Foote.** 1997. Resistance to *Leishmania major* is linked to the H2 region on chromosome 17 and to chromosome 9. J. Exp. Med. **185:**1–6.
18. **Sacks, D., and N. Noben-Trauth.** 2002. The immunology of susceptibility and resistance to *Leishmania major* in mice. Nat. Rev. Immunol. **2:**845–858.
19. **Sacks, D. L., and R. P. da Silva.** 1987. The generation of infective stage *Leishmania major* promastigotes is associated with the cell-surface expression and release of a developmentally regulated glycolipid. J. Immunol. **139:**3099–3106.
20. **Sacks, D. L., and P. V. Perkins.** 1984. Identification of an infective stage of *Leishmania* promastigotes. Science **223:**1417–1419.
21. **Shaffer, J. P.** 1995. Multiple hypothesis testing. Annu. Rev. Psychol. 561–576.
22. **Solbach, W., and T. Laskay.** 2000. The host response to *Leishmania* infection. Adv. Immunol. **74:**275–317.
23. **Titus, R. G., M. Marchand, T. Boon, and J. A. Louis.** 1985. A limiting dilution assay for quantifying *Leishmania major* in tissues of infected mice. Parasite Immunol. **7:**545–555.
24. **Walton, B. C., and L. Valverde.** 1979. Racial differences in espundia. Ann. Trop. Med. Parasitol. **73:**23–29.

Editor: W. A. Petri, Jr.